



CHALMERS
UNIVERSITY OF TECHNOLOGY

Giant-atom effects on population and entanglement dynamics of Rydberg atoms in the optical regime

Downloaded from: <https://research.chalmers.se>, 2026-03-17 01:15 UTC

Citation for the original published paper (version of record):

Chen, Y., Du, L., Zhang, Y. et al (2023). Giant-atom effects on population and entanglement dynamics of Rydberg atoms in the optical regime. *Physical Review Research*, 5(4). <http://dx.doi.org/10.1103/PhysRevResearch.5.043135>

N.B. When citing this work, cite the original published paper.

Giant-atom effects on population and entanglement dynamics of Rydberg atoms in the optical regime

Yao-Tong Chen¹, Lei Du^{2,*}, Yan Zhang¹, Lingzhen Guo³, Jin-Hui Wu^{1,†}, M. Artoni^{4,5} and G. C. La Rocca⁶

¹*School of Physics and Center for Quantum Sciences, Northeast Normal University, Changchun 130024, China*


²*Department of Microtechnology and Nanoscience, Chalmers University of Technology, 41296 Gothenburg, Sweden*

³*Center for Joint Quantum Studies and Department of Physics, School of Science, Tianjin University, Tianjin 300072, China*

⁴*Department of Chemistry and Physics of Materials, University of Brescia, 25133 Brescia, Italy*

⁵*European Laboratory for Non-Linear Spectroscopy, 50019 Sesto Fiorentino, Italy*

⁶*NEST, Scuola Normale Superiore, Piazza dei Cavalieri 7, I-56126 Pisa, Italy*

 (Received 28 April 2023; revised 10 July 2023; accepted 5 October 2023; published 9 November 2023)

Giant atoms are attracting interest as an emerging paradigm in the quantum optics of engineered waveguides. At variance with the well-known artificial giant atoms for microwave photonics, here we propose the archetype of a giant atom working in the optical regime by considering a pair of interacting Rydberg atoms coupled to a photonic crystal waveguide (PCW) and also driven by a coherent field. Giant-atom effects are observed as a phase-dependent decay of the double Rydberg excitation during the initial evolution stage while a nontrivial internal entanglement is exhibited at later times. Such an entanglement onset occurs in the presence of intrinsic atomic decay toward nonguided vacuum modes and is accompanied by antibunching in the emitted photons. Our predictions should be observable in current Rydberg-PCW experiments and may open the way toward giant-atom optical photonics for quantum information processing.

DOI: [10.1103/PhysRevResearch.5.043135](https://doi.org/10.1103/PhysRevResearch.5.043135)

I. INTRODUCTION

A fascinating paradigm of quantum optics dubbed “giant atom” has been developed recently to describe situations where artificial atoms interact with microwave or acoustic fields beyond the standard dipole approximation [1]. With state-of-the-art technologies, one can implement giant atoms that are coupled to a waveguide at multiple points, with coupling separations comparable to field wavelengths. These nonlocal interactions can result in peculiar self-interference effects, which account for a number of phenomena not happening in conventional natural atoms, such as frequency-dependent atomic relaxation rates and Lamb shifts [2–6], nonexponential atomic decay [7–9], in-band decoherence-free interactions [3,10–12], and exotic atom-photon bound states [13–18]. To date, platforms capable of implementing giant atoms mainly include superconducting quantum circuits [3,8,19,20], coupled waveguide arrays [21], and matter waves in optical lattices [22], but have also been extended to synthetic frequency dimensions [23] and ferromagnetic spin systems as an alternative [24].

Nevertheless, it is important to explore new physics of giant atoms within different atomic architectures, especially

those working with natural atoms and optical photons beyond the microwave regime. Rydberg atoms, unlike those in low-lying excited states, exhibit unique properties including strong dipole-dipole interactions and long radiative lifetimes [25] and turn out to be an excellent building block in quantum information processing, with potential applications for realizing quantum logic gates [26–29], single-photon sources [30–33], and various entangled states [34–37]. Rydberg atoms have also been successfully employed in waveguide quantum electrodynamics by coupling to engineered structures like optical nanofibers [38], photonic crystal waveguides [39], and coplanar microwave waveguides [40].

In this paper, we study giant-atom effects in the optical regime by considering a pair of two-level Rydberg atoms coupled to a photonic crystal waveguide (PCW) through the two lower transitions and driven by a coherent field through the two upper transitions (see Fig. 1). A typical self-interference effect appears at *shorter times* of the atomic pair’s dynamic evolution dominated by two competing two-photon resonant transitions, thereby realizing a *synthetic* giant atom with two coupling points at a variable distance d about the atomic separation R . For *longer times*, we observe instead internal entanglement onset through mutual Rydberg excitations of the two atoms as the phase ϕ accumulated from a coupling point to the other takes specific values, which depend on d hence tunable. This effect is characterized by a detailed examination on *quantum correlations* of the emitted photons and further understood in terms of *dark states* decoupled from both coherent field and waveguide modes. These results hold also for continuous atom-waveguide couplings, which are more appropriate to the large spatial extents of Rydberg atoms.

*lei.du@chalmers.se

†jhwu@nenu.edu.cn

Published by the American Physical Society under the terms of the [Creative Commons Attribution 4.0 International](https://creativecommons.org/licenses/by/4.0/) license. Further distribution of this work must maintain attribution to the author(s) and the published article’s title, journal citation, and DOI.

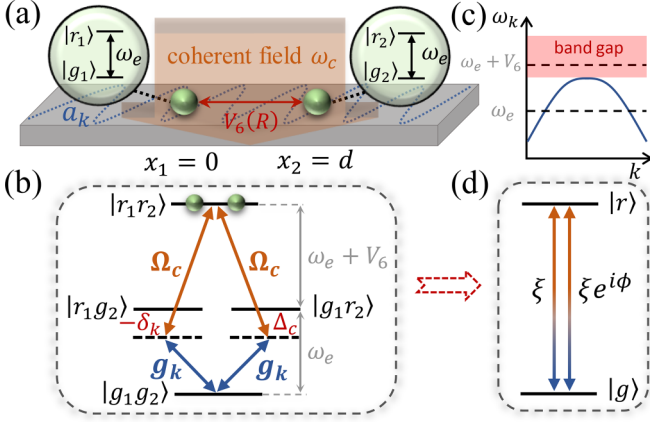


FIG. 1. (a) The two-level configuration (*single-atom basis*). Two Rydberg atoms placed at a distance R interact via a potential $V_6(R)$ and couple to a waveguide mode a_k at $x_1 = 0$ or $x_2 = d$ while driven by a coherent field ω_c . (b) The four-level configuration (*two-atom basis*). Blue (red) lines represent single (double) Rydberg excitations, whereby two lower (upper) transitions are coupled by mode a_k of strength g_k (field ω_c of strength Ω_c). (c) The dispersion relation of a PCW: frequency ω_e of the lower transitions falls within the propagating band while frequency $\omega_e + V_6$ of the upper transitions falls within the band gap (red shaded). (d) The (equivalent) synthetic two-level giant atom with $|g\rangle \equiv |g_1g_2\rangle$ and $|r\rangle \equiv |r_1r_2\rangle$, upon adiabatic elimination of the single-excitation states, bears separate couplings of strengths ξ at x_1 and $\xi e^{i\phi}$ at x_2 , with ϕ being the accumulated phase between x_1 and x_2 .

II. MODEL

We start by illustrating in Fig. 1(a) the model of a pair of Rydberg atoms with ground $|g_{1,2}\rangle$ and Rydberg $|r_{1,2}\rangle$ states separated by frequency ω_e and trapped in the vicinity of a PCW [41,42] at $x_1 = 0$ and $x_2 = d$, respectively. The two atoms are illuminated by a coherent field of frequency ω_c and interact through a (repulsive) van der Waals (vdW) potential $V_6 = C_6/R^6$, when *both* are excited to the Rydberg states, with C_6 being the vdW coefficient and R the interatomic distance, which could be different from d (see Appendix A for details). The vdW interaction results in the shifted energy $2\hbar\omega_e + \hbar V_6$ for the *double-excitation* state $|r_1r_2\rangle$ while the *single-excitation* states $|r_1g_2\rangle$ and $|g_1r_2\rangle$ remain to exhibit energy $\hbar\omega_e$. In the two-atom basis, for a large enough V_6 , we have the four-level configuration shown in Fig. 1(b) whereby the coherent field ω_c drives only transitions $|g_1r_2\rangle \leftrightarrow |r_1r_2\rangle$ and $|r_1g_2\rangle \leftrightarrow |r_1r_2\rangle$ with detuning $\Delta_c = \omega_c - (\omega_e + V_6)$ and strength Ω_c , while a waveguide mode of frequency ω_k (wavevector k) drives only transitions $|g_1g_2\rangle \leftrightarrow |g_1r_2\rangle$ and $|g_1g_2\rangle \leftrightarrow |r_1g_2\rangle$ with detuning $\delta_k = \omega_k - \omega_e$ and strength g_k . This scheme is supported by the following two considerations. *First*, ω_c is far away from ω_e but close to $\omega_e + V_6$ with $\Delta_c \ll V_6$, so that the coherent field can only drive two upper transitions. *Second*, ω_e and $\omega_e + V_6$ fall, respectively, within the lower propagating band and the band gap of a PCW as sketched in Fig. 1(c), so that the waveguide mode can only drive the two lower transitions.

Then, for a continuum of waveguide modes interacting only with two lower transitions, the Hamiltonian in the

rotating-wave approximation is ($\hbar = 1$)

$$H = \omega_e(\sigma_+^1\sigma_-^1 + \sigma_+^2\sigma_-^2) + (\omega_e + V_6/2)(\sigma_+^3\sigma_-^3 + \sigma_+^4\sigma_-^4) + \int dk \omega_k a_k^\dagger a_k + \left[\int dk g a_k (\sigma_+^1 + e^{ikd} \sigma_+^2) + \Omega_c e^{-i\omega_c t} (\sigma_+^3 + \sigma_+^4) + \text{H.c.} \right]. \quad (1)$$

Here, we have introduced the atomic raising operators $\sigma_+^1 = |r_1g_2\rangle\langle g_1g_2|$, $\sigma_+^2 = |g_1r_2\rangle\langle g_1g_2|$, $\sigma_+^3 = |r_1r_2\rangle\langle r_1g_2|$, and $\sigma_+^4 = |r_1r_2\rangle\langle g_1r_2|$ (two-atom basis) while the corresponding lowering operators are $\sigma_-^j = (\sigma_+^j)^\dagger$. Moreover, a_k^\dagger and a_k refer, respectively, to the creation and annihilation operators of a waveguide mode ω_k . We have also assumed constant coupling strengths, i.e., $g_k \simeq g$, in the Weisskopf-Wigner approximation.

As we address only the two-atom dynamics, the waveguide modes of density $D(k)$ at frequency ω_k can be traced out (Born-Markov approximation), yielding the master equation for density operator ρ [43,44] (see Appendix B for details),

$$\partial_t \rho = -i[H_{at}, \rho] + \sum_{i=1}^4 \gamma \mathcal{L}[\sigma_-^i] \rho + \sum_{j=1}^2 \Gamma \mathcal{L}[\sigma_-^j] \rho + \Gamma_{ex} \left[\left(\sigma_-^1 \rho \sigma_+^2 - \frac{1}{2} \{ \sigma_+^1 \sigma_-^2, \rho \} \right) + \text{H.c.} \right], \quad (2)$$

where $\mathcal{L}[O]\rho = O\rho O^\dagger - \frac{1}{2}\{O^\dagger O, \rho\}$ is the Lindblad super-operator describing two-atom decay processes, with $\Gamma(k) = 4\pi g^2 D(k)$ denoting the decay rate into relevant modes of the waveguide (guided modes) [2,3] while γ being the mean decay rate into other electromagnetic modes (nonguided modes). Under the two-photon resonance condition $\Delta_c + \delta_k \simeq 0$, assumed to hold for all guided modes, the atomic Hamiltonian is

$$H_{at} = \Delta_c(\sigma_+^1\sigma_-^1 + \sigma_+^2\sigma_-^2) + J_{ex}(\sigma_+^1\sigma_-^2 + \sigma_+^2\sigma_-^1)/2 + [\Omega_c(\sigma_+^3 + \sigma_+^4) + \text{H.c.}], \quad (3)$$

with $J_{ex} = \Gamma \sin\phi$ and $\Gamma_{ex} = \Gamma \cos\phi$ denoting, respectively, the *coherent* and *dissipative* parts of the exchange interaction mediated by the waveguide. Here we have defined $\phi(k) = |k|d = \omega_k d / |v_g(k)| \simeq \omega_e d / |v_g(k)|$ with $v_g(k)$ being the group velocity of a guided mode with a “linearized” dispersion $\omega_k \simeq kv_g(k)$. It is worth stressing that Γ_{ex} serves as a reservoir to *engineer* the atomic decay through selected guided modes ω_k (or bandwidth of modes) and their density distribution $D(k)$. In turn, such an engineered reservoir together with the atomic separation d represents a set of knobs to control the phase $\phi(k)$ acquired by an emitted photon between the *contact points* x_1 and x_2 of a giant atom (see below).

III. SYNTHETIC TWO-LEVEL GIANT ATOM: THE SHORT-TIME REGIME

Maintaining $\Delta_c + \delta_k \simeq 0$ and further requiring $|\Delta_c| \gg \Omega_c, g$, the two atoms initially in the double Rydberg state $|r_1r_2\rangle$ would behave like a two-level giant atom decaying directly to the ground state $|g_1g_2\rangle$ at two coupling points

x_1 and x_2 . This expectation will be verified by numerically comparing the dynamics of the four-level atomic pair to that of the synthetic two-level giant atom. In the latter picture, the two atoms interact with the waveguide modes only through the two-photon resonant transition $|r_1 r_2\rangle \leftrightarrow |g_1 g_2\rangle$ whereby an external photon of frequency ω_c and a waveguide photon of frequency ω_k are emitted (or absorbed) at the same time. Upon the adiabatic elimination of states $|r_1 g_2\rangle$ and $|g_1 r_2\rangle$ [45,46], the effective $|r_1 r_2\rangle \leftrightarrow |g_1 g_2\rangle$ transition amplitude consists of two contributions: $\xi_1 = -g\Omega_c/\Delta_c \equiv \xi$ (interaction at $x_1 = 0$) and $\xi_2 = \xi e^{i\phi}$ (interaction at $x_2 = d$), as sketched in Fig. 1(d), which interfere with each other.

With the above assumptions, we write down the synthetic two-level giant-atom Hamiltonian as

$$\mathcal{H} = (2\omega_e + V_6)\sigma_+\sigma_- + \int dk(\omega_k + \omega_c)a_k^\dagger a_k + \int dk[\xi a_k(1 + e^{ikd})\sigma_+ + \text{H.c.}], \quad (4)$$

in terms of the transition operator $\sigma_+ = (\sigma_-)^\dagger = |r\rangle\langle g|$ with $|r\rangle \equiv |r_1 r_2\rangle$ and $|g\rangle \equiv |g_1 g_2\rangle$. Again, by tracing out the waveguide modes, we arrive at the master equation for the giant-atom density operator ρ (see Appendix C for details)

$$\partial_t \rho = 2\gamma \mathcal{L}[\sigma_-]\rho + (\Upsilon + \Upsilon^*)\sigma_- \rho \sigma_+ - \Upsilon \sigma_+ \sigma_- \rho - \Upsilon^* \rho \sigma_+ \sigma_-, \quad (5)$$

where $\Upsilon = 4\pi\xi^2 D(1 + e^{i\phi}) = (\Gamma + \Gamma_{ex} + iJ_{ex})\Omega_c^2/\Delta_c^2$ with its real and imaginary parts being, respectively, the phase-dependent decay rate and Lamb shift.

In the remaining part, we perform numerical analysis in support of the predictions anticipated above. We first consider that for large enough (driving) detunings $|\Delta_c|$, the adiabatic elimination of two single-excitation states can be actually made, providing in turn an adequate evidence of the equivalence between the (four-level) atomic pair and the (two-level) giant atom in the short-time regime. This has been examined in Fig. 2(a) by comparing time evolutions of atomic-pair population $\rho_{r_1 r_1, r_2 r_2}$ based on Eq. (2) and giant-atom population ρ_{rr} based on Eq. (5) with matched parameters. Taking $\phi = 40.5\pi$ as an example and starting from $\rho_{r_1 r_1, r_2 r_2}(0) = \rho_{rr}(0) = 1$, we find that $\rho_{r_1 r_1, r_2 r_2}(t)$ and $\rho_{rr}(t)$ exhibit a better agreement for a larger $|\Delta_c|$ so that the adiabatic elimination leading to a giant atom becomes reliable for $|\Delta_c|/\Omega_c \gtrsim 30$. It is also worth noting that $\rho_{r_1 r_1, r_2 r_2}(t)$ and $\rho_{rr}(t)$ decay faster as $|\Delta_c|$ decreases because a smaller $|\Delta_c|$ results in a stronger coupling strength ξ and thereby a larger decay rate $\text{Re}(\Upsilon)$ of the synthetic giant atom.

The giant-atom self-interference effect can instead be examined by plotting $\rho_{r_1 r_1, r_2 r_2}(t)$ in Fig. 2(b) for $\Delta_c = 30$ MHz and different values of ϕ . It is clear that an enhanced (reduced) decay occurs for $\rho_{r_1 r_1, r_2 r_2}(t)$ in the case of $\phi = 2m\pi$ ($\phi = 2m\pi + \pi$) with $m \in \mathbb{Z}$ due to a perfectly constructive (destructive) interference between two coupling points, as can be seen from $\text{Im}(\Upsilon) = 0$ and $\text{Re}(\Upsilon) = \Gamma(1 + \cos\phi)\Omega_c^2/\Delta_c^2$. The atomic pair is found in particular to show an undamped double-excitation population [$\rho_{r_1 r_1, r_2 r_2}(t) \equiv 1$] for $\phi = 2m\pi + \pi$ and $\gamma = 0$, which is one of the most remarkable features of giant atoms [2] due to a complete decoupling from the waveguide ($\Upsilon = 0$) and a vanishing

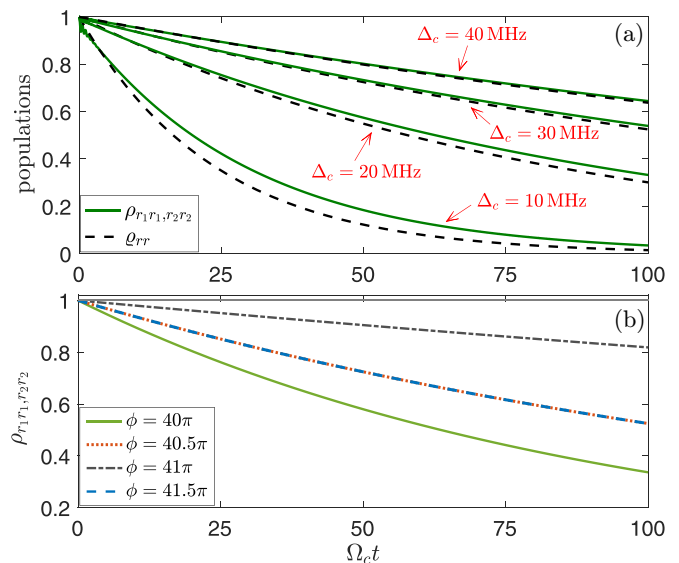


FIG. 2. (a) Time evolutions of double Rydberg population $\rho_{r_1 r_1, r_2 r_2}$ and giant-atom population ρ_{rr} with $\phi = 40.5\pi$ and different values of Δ_c . (b) Time evolutions of $\rho_{r_1 r_1, r_2 r_2}$ with $\Delta_c = 30$ MHz and different values of ϕ . Other parameters are $V_6 = 20$ GHz, $\Omega_c = 1.0$ MHz, $\Gamma = 1.0$ MHz, and $\gamma = 1.0$ kHz. The thin gray line in (b) is shown as a reference for $\gamma = 0$ (no intrinsic decay) with $\Delta_c = 30$ MHz and $\phi = 41\pi$.

intrinsic decay ($\gamma = 0$). In the case of $\phi = 2m\pi \pm \pi/2$, we have $\text{Im}(\Upsilon) = \pm\Gamma\Omega_c^2/\Delta_c^2$ and $\text{Re}(\Upsilon) = \Gamma\Omega_c^2/\Delta_c^2$, which accounts for the identical population dynamics with a moderate decay since opposite detunings (Lamb shifts) make no difference.

We finally detail how one can actually adjust phase ϕ while leaving V_6 unchanged. To this end, a pair of ^{87}Rb atoms with ground state $|g_{1,2}\rangle = |5S_{1/2}, F = 2, m_F = 2\rangle$ and Rydberg state $|r_{1,2}\rangle = |75P_{3/2}, m_J = 3/2\rangle$ of transition frequency $\omega_e \simeq 2\pi \times 1009$ THz are taken here as an example. In this case, we have $\gamma \simeq 1.0$ kHz for the intrinsic Rydberg lifetime $\tau \simeq 964$ μs while $V_6 \simeq 20$ GHz for $R \simeq 3.1$ μm and $C_6 \simeq 2\pi \times 2.8 \times 10^{12} \text{s}^{-1} \mu\text{m}^6$ [47,48]. When the atomic pair is placed exactly along the waveguide, we have $d = R$ and hence $\phi \simeq 41.6\pi$ by assuming here that v_g is a half of the vacuum light speed c . When the atomic pair is misaligned along the waveguide, however, we attain $d \simeq 2.95$ μm and hence $\phi \simeq 39.6\pi$ with neither R nor V_6 being changed (see Appendix A).

IV. ATOMIC ENTANGLEMENT ONSET: THE LONG-TIME REGIME

Now leaving the short-time regime where the atomic pair can be modeled as a giant atom according to Eq. (5), we turn to the long-time regime where the decay toward nonguided vacuum modes becomes important as less and less population can be found in the double-excitation state. A peculiar aspect of the long-time regime is the internal entanglement of the atomic pair (i.e., a specific superposition of two single-excitation states) generated by the coherent interaction described by H_{at} , which can be quantified by the Wootters

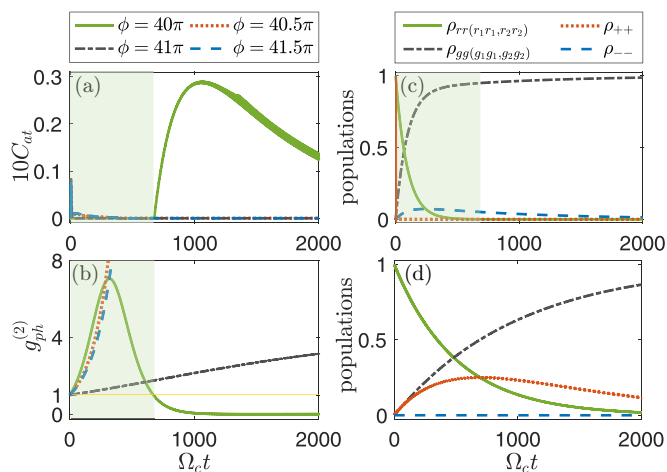


FIG. 3. Time evolutions of atomic concurrence C_{at} (a) and photonic correlation $g_{ph}^{(2)}$ (b) for different values of ϕ as well as atomic populations ρ_{gg} , ρ_{rr} , ρ_{++} , and ρ_{--} for $\phi = 40\pi$ (c) and $\phi = 41\pi$ (d) with other parameters same as in Fig. 2(b).

concurrence [49–51]

$$C_{at} = \text{Max}(0, \lambda_1 - \lambda_2 - \lambda_3 - \lambda_4) \quad (6)$$

with $\lambda_1 > \lambda_2 > \lambda_3 > \lambda_4$ being the four eigenvalues of matrix X defined by $X^2 = \sqrt{\rho}(\sigma_y \otimes \sigma_y)\rho^*(\sigma_y \otimes \sigma_y)\sqrt{\rho}$ and the standard Pauli matrix σ_y . This concurrence takes values in the range of $[0,1]$ with $C_{at} = 0$ ($C_{at} = 1$) denoting a nonentangled (maximally entangled) state and is related to the correlation function [52–54]

$$g_{ph}^{(2)} = \frac{\rho_{r_1 r_1, r_2 r_2}}{\rho_{r_1 r_1} \rho_{r_2 r_2}} \quad (7)$$

of the photons emitted by two Rydberg atoms. As usual, $\rho_{r_1 r_1} = \langle r_1 | \text{Tr}_2 \rho | r_1 \rangle$ and $\rho_{r_2 r_2} = \langle r_2 | \text{Tr}_1 \rho | r_2 \rangle$ are obtained from the reduced density matrices of different atoms, while $g_{ph}^{(2)} > 1$ and $g_{ph}^{(2)} < 1$ refer to the effects of photon bunching and anti-bunching, respectively.

We plot in Fig. 3(a) time evolutions of C_{at} for different values of ϕ starting from the same double-excitation state and find that C_{at} becomes suddenly nonzero at a critical time for $\phi = 2m\pi$ but remains vanishing for other values of ϕ . Such an onset of internal atomic entanglement happens when the photon correlation function $g_{ph}^{(2)}$ evolves from the regime of bunching to that of antibunching as shown in Fig. 3(b), making a clear connection between the emergence of photon antibunching effect and the generation of internal atomic entanglement.

It is worth noting that $g_{ph}^{(2)}$ also indicates how the two Rydberg atoms are distributed in the single- and double-excitation states, which provides a better understanding of the physics of the entanglement sudden-onset dynamics. This inspires us to further plot ρ_{gg} , ρ_{rr} , ρ_{++} , and ρ_{--} in Fig. 3(c) for $\phi = 2m\pi$ and Fig. 3(d) for $\phi = 2m\pi + \pi$ with $|g\rangle \equiv |g_1 g_2\rangle$, $|r\rangle \equiv |r_1 r_2\rangle$, and $|\pm\rangle \equiv 1/\sqrt{2}(|r_1 g_2\rangle \pm |g_1 r_2\rangle)$ by considering that $|+\rangle$ ($|-\rangle$) is the symmetric (antisymmetric) dressed state of H_{at} in the case of $\phi = m\pi$ due to $J_{ex} = 0$. To be more specific, we have the following dynamic equations

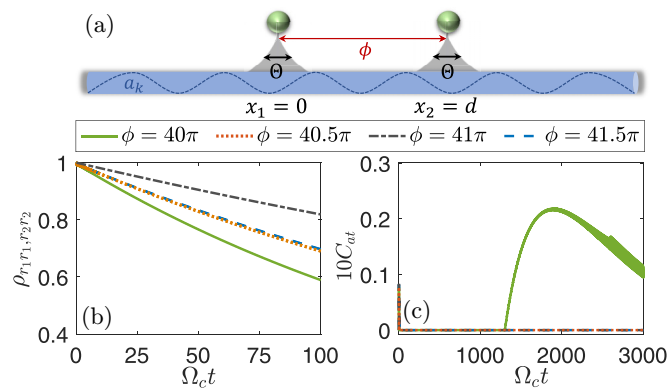


FIG. 4. (a) Schematic of two Rydberg atoms close to a waveguide with identical exponential coupling distributions around $x_1 = 0$ and $x_2 = d$. Time evolutions of population $\rho_{r_1 r_1, r_2 r_2}$ (b) and concurrence C_{at} (c) with $\Theta = 5\pi/2$ and different values of ϕ . Other parameters are the same as in Fig. 2(b).

(see Appendix B for calculation details):

$$\begin{aligned} \partial_t \rho_{++} &= -\gamma_+ \rho_{++} + \gamma \rho_{rr} + i\Omega_c^* \rho_{r+} - i\Omega_c \rho_{+r}, \\ \partial_t \rho_{--} &= -\gamma_- \rho_{--} + \gamma \rho_{rr}, \end{aligned} \quad (8)$$

with $\gamma_{\pm} = \gamma + \Gamma \pm \Gamma_{ex}$. It is clear that $|-\rangle$ is decoupled from field Ω_c and will become a *dark* state if it is further immune to the waveguide modes in the case of $\phi = 2m\pi$. However, $|+\rangle$ is always a *bright* state in that its dynamics depends on field Ω_c all the time.

Note in particular that $\gamma_+ = \gamma + 2\Gamma \gg \gamma_- = \gamma$ in the case of $\phi = 2m\pi$, which explains why ρ_{++} vanishes while ρ_{--} does not in Fig. 3(c) so that we have $g_{ph}^{(2)} \simeq 4\rho_{rr}/\rho_{--}^2$. The atomic entanglement onset occurs for $\phi = 2m\pi$ just because a dark state immune to field Ω_c allows the transition from $4\rho_{rr} > \rho_{--}^2$ to $4\rho_{rr} < \rho_{--}^2$. In the case of $\phi = 2m\pi + \pi$, however, we have a nonzero ρ_{++} and a vanishing ρ_{--} in Fig. 3(d) and hence $g_{ph}^{(2)} \simeq 4\rho_{rr}/\rho_{++}^2$ due to $\gamma_- = \gamma + 2\Gamma \gg \gamma_+ = \gamma$. The atomic entanglement onset is absent for $\phi = 2m\pi + \pi$ just because a bright state interacting with field Ω_c always results in $4\rho_{rr} > \rho_{++}^2$. Finally, we stress that the fact of $\rho_{++} > 0$ ($\rho_{--} > 0$) and $\rho_{--} = 0$ ($\rho_{++} = 0$) does not mean that the decomposition of a mixed state ρ must include a pure state $|+\rangle$ ($|-\rangle$), hence does not mean that we must have $C_{at} > 0$, which further explains why C_{at} could suddenly become nonzero only for $\phi = 2m\pi$.

V. CONTINUOUS COUPLINGS

Working with “point-like” atom-waveguide couplings, as assumed so far, is just a rough approximation for highly-excited Rydberg states of size $\bar{r} \propto n^2$, with n being the principal quantum number. We then extend our discrete-coupling configuration results to the continuum limit whereby the coupling region becomes a large ensemble of coupling points, each with a different strength. For an exponential continuous distribution [4,55] of such coupling strengths spread about each contact point with a characteristic width Θ as in Fig. 4(a), we find that the master equations (2) and (5) can be generalized to the continuous-coupling limit by replacing $\{\Gamma, \Gamma_{ex}, J_{ex}, \Upsilon\}$ with $\{\Gamma', \Gamma'_{ex}, J'_{ex}, \Upsilon'\}$ and meanwhile

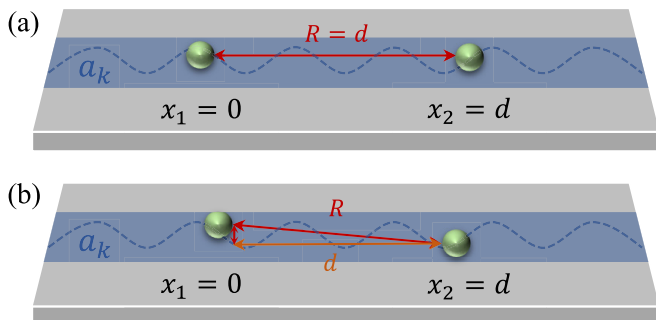


FIG. 5. Arrangement details of two Rydberg atoms with respect to a one-dimensional waveguide shown as a blue area. The atomic pair is (a) placed along the waveguide with $d = R$ or (b) misaligned along the waveguide with $d < R$.

introducing an interaction term $J'(\sigma_+^1\sigma_-^1 + \sigma_+^2\sigma_-^2)$ in Eq. (3). While explicit expressions of Γ' , Γ'_{ex} , J'_{ex} , Υ' , and J' are given in Appendix D, here we use them to plot in Figs. 4(b) and 4(c) the time evolutions of $\rho_{r_1r_1, r_2r_2}$ and C_{at} in the short-time and long-time regimes, respectively, for different values of ϕ and a fixed Θ .

It is easy to see that the giant-atom effects of phase-dependent population decay and entanglement onset remain observable for a remarkable coupling broadening. Moreover, the dynamic behavior of $\rho_{r_1r_1, r_2r_2}$ for $\Theta = 5\pi/2$ (continuous couplings) is identical to that for $\Theta = 0$ (point-like couplings) in the case of $\phi = 2m\pi + \pi$ since there is no decay toward the waveguide with $\text{Re}(\Upsilon') = 0$. Note, however, that a nonzero Lamb shift with $\text{Im}(\Upsilon') \neq 0$ always exists for continuous couplings (see Appendix D), which does not affect atomic population decay but would be relevant to other problems such as photon scattering.

VI. CONCLUSIONS

We have proposed a feasible scheme for constructing a synthetic giant atom with a pair of interacting Rydberg atoms coupled to an optical PCW. Compared to well-known platforms involving microwave photons (e.g., superconducting quantum circuits [3,8]) or a recent matter-wave analogy [22], our Rydberg-pair giant-atom platform is clearly suitable for manipulating optical photons. Giant-atom effects manifest

themselves through a phase-dependent population dynamics in the short-time regime whereas an internal entanglement onset at longer times. The latter differs also from a recently examined entanglement generation taking place between two giant atoms in the microwave regime [51].

The giant-atom effects we anticipate here are observable also for *continuous* couplings, indicating their robustness against unavoidable coupling broadenings, and could be extended to *multi-pairs* of Rydberg atoms when coupled to a meandering waveguide [56]. These features make our platform altogether suitable to explore regimes that cannot be reached with microwave systems and also well poised to potential applications in the optical network engineering and information processing.

ACKNOWLEDGMENTS

This work is supported by the National Natural Science Foundation of China (Grant No. 12074061), the National Key Research and Development Program of China (Grant No. 2021YFE0193500), the Italian PNRR MUR (Project PE0000023-NQSTI), and the ‘‘Fondo per le attivit a a carattere internazionale’’ of The University of Brescia for the year 2023.

APPENDIX A: MISALIGNED ARRANGEMENT OF TWO ATOMS ALONG A WAVEGUIDE

In this section, we discuss how to manipulate the van der Waals (vdW) potential V_6 and the accumulated phase ϕ separately. As mentioned in the main text, V_6 and ϕ are determined by the (straight-line) distance R between a pair of Rydberg atoms and the separation d (along the waveguide) between two coupling points, respectively. When this atomic pair is placed exactly along the waveguide, we have $R \equiv d$ so that ϕ or V_6 cannot be changed alone as shown in Fig. 5. In this case, it is easy to attain $\phi \simeq \omega_e d/v_g = \omega_e R/v_g = 41.6\pi$ with $R \simeq 3.1 \mu\text{m}$, $\omega_e \simeq 2\pi \times 1009 \text{ THz}$, and $v_g \simeq 0.5c$ as considered in the main text. In order to change ϕ and V_6 separately, we can choose a *misaligned* arrangement of this atomic pair as shown in Fig. 5, where d is clearly smaller than R . In this case, keeping $R \simeq 3.1 \mu\text{m}$ and hence $V_6 = 20 \text{ GHz}$ unchanged, it is viable to tune ϕ in the range of $[41.6, 39.6]\pi$ by reducing d from $3.1 \mu\text{m}$ with a vanishing misaligned angle to $2.95 \mu\text{m}$ with a 0.09π misaligned angle.

APPENDIX B: MASTER EQUATION OF A TWO-ATOM FOUR-LEVEL CONFIGURATION

In this section, we provide the derivation procedures from Eq. (1) on Hamiltonian H to Eq. (2) on density operator ρ in the main text. As shown in Fig. 1(b), two upper transitions $|g_1r_2\rangle \leftrightarrow |r_1r_2\rangle$ and $|r_1g_2\rangle \leftrightarrow |r_1r_2\rangle$ are driven by the external coherent field Ω_c while two lower transitions $|g_1g_2\rangle \leftrightarrow |g_1r_2\rangle$ and $|g_1g_2\rangle \leftrightarrow |r_1g_2\rangle$ are coupled to the waveguide modes. Under the two-photon resonance condition (i.e., $\Delta_c \simeq -\delta_k$ with $\Delta_c = \omega_c - \omega_e - V_6$ and $\delta_k = \omega_k - \omega_e$), we neglect the interactions resulted from coherent field ω_c in H for the moment and move to the interaction picture with respect to $H_0 = (2\omega_e + V_6 - \omega_c)(\sigma_+^1\sigma_-^1 + \sigma_+^2\sigma_-^2) + \int dk \omega_k a_k^\dagger a_k = (\omega_e - \Delta_c)(\sigma_+^1\sigma_-^1 + \sigma_+^2\sigma_-^2) + \int dk \omega_k a_k^\dagger a_k$. Then the Hamiltonian describing the atom-waveguide interaction can be written as

$$\begin{aligned} H_{\text{int}}(t) &= \int_{-\infty}^{+\infty} dk [g e^{-i(\Delta_c + \omega_k - \omega_e)t} a_k \sigma_+^1 + g e^{ikd} e^{-i(\Delta_c + \omega_k - \omega_e)t} a_k \sigma_+^2 + \text{H.c.}] \\ &= \int_{-\infty}^{+\infty} dk [g e^{-i(\Delta_c + \delta_k)t} a_k \sigma_+^1 + g e^{ikd} e^{-i(\Delta_c + \delta_k)t} a_k \sigma_+^2 + \text{H.c.}] \end{aligned} \quad (\text{B1})$$

with $\sigma_+^1 = (\sigma_-^1)^\dagger = |r_1g_2\rangle\langle g_1g_2|$ and $\sigma_+^2 = (\sigma_-^2)^\dagger = |g_1r_2\rangle\langle g_1g_2|$ defined as in the main text.

To study the population dynamics of this atomic pair, we can eliminate the waveguide field via a standard procedure and calculate the following master equation for a reduced density operator [43,44]

$$\partial_t \rho(t) = - \int_0^\infty d\tau \text{Tr}_w [H_{\text{int}}(t), [H_{\text{int}}(t - \tau), \rho_w \otimes \rho(t)]], \quad (\text{B2})$$

where Tr_w represents a partial tracing over the waveguide degrees of freedom and $\rho_w = |0\rangle\langle 0|$ is the *initial* vacuum state of the waveguide modes. Substituting Eq. (B1) into Eq. (B2) we have

$$\begin{aligned} \partial_t \rho &= \sum_{j=1,2} \Gamma \left(\sigma_{-}^j \rho \sigma_{+}^j - \frac{1}{2} \sigma_{+}^j \sigma_{-}^j \rho - \frac{1}{2} \rho \sigma_{+}^j \sigma_{-}^j \right) + \frac{\tilde{\Gamma} + \tilde{\Gamma}^*}{2} (\sigma_{-}^1 \rho \sigma_{+}^2 + \sigma_{-}^2 \rho \sigma_{+}^1) \\ &\quad - \frac{\tilde{\Gamma}}{2} (\sigma_{+}^1 \sigma_{-}^2 \rho + \sigma_{+}^2 \sigma_{-}^1 \rho) - \frac{\tilde{\Gamma}^*}{2} (\rho \sigma_{+}^1 \sigma_{-}^2 + \rho \sigma_{+}^2 \sigma_{-}^1) \\ &= \sum_{j=1,2} \Gamma \left(\sigma_{-}^j \rho \sigma_{+}^j - \frac{1}{2} \sigma_{+}^j \sigma_{-}^j \rho - \frac{1}{2} \rho \sigma_{+}^j \sigma_{-}^j \right) + \Gamma_{\text{ex}} (\sigma_{-}^1 \rho \sigma_{+}^2 + \sigma_{-}^2 \rho \sigma_{+}^1) \\ &\quad - \frac{\Gamma_{\text{ex}}}{2} (\sigma_{+}^1 \sigma_{-}^2 \rho + \sigma_{+}^2 \sigma_{-}^1 \rho + \rho \sigma_{+}^1 \sigma_{-}^2 + \rho \sigma_{+}^2 \sigma_{-}^1) - \frac{iJ_{\text{ex}}}{2} (\sigma_{+}^1 \sigma_{-}^2 \rho + \sigma_{+}^2 \sigma_{-}^1 \rho - \rho \sigma_{+}^1 \sigma_{-}^2 - \rho \sigma_{+}^2 \sigma_{-}^1), \end{aligned} \quad (\text{B3})$$

with

$$\begin{aligned} \Gamma &= 2g^2 \int_0^\infty d\tau \int_{-\infty}^{+\infty} dke^{\pm i(\Delta_c + \delta_k)\tau} = 2g^2 \int_0^\infty d\tau e^{\pm i\Delta_c \tau} \left(\int_{-\infty}^0 dke^{\pm i\delta_k \tau} + \int_0^{+\infty} dke^{\pm i\delta_k \tau} \right) \\ &= \frac{4g^2}{v_g} \int_0^\infty d\tau e^{\pm i\Delta_c \tau} \int_{-\infty}^{+\infty} d\delta_k e^{\pm i\delta_k \tau} = \frac{4g^2}{v_g} \int_0^\infty d\tau e^{\pm i\Delta_c \tau} 2\pi \delta(\tau) = \frac{4\pi g^2}{v_g} = 4\pi g^2 D(k), \\ \tilde{\Gamma} &= 2g^2 \int_0^\infty d\tau \int_{-\infty}^{+\infty} dke^{-i(\Delta_c + \delta_k)\tau} e^{\pm ikd} \\ &= 2g^2 \int_0^\infty d\tau \left[\int_{-\infty}^0 dke^{-i(\Delta_c + \delta_k)\tau} e^{\mp i(\delta_k + \omega_e)d/v_g} + \int_0^{+\infty} dke^{-i(\Delta_c + \delta_k)\tau} e^{\pm i(\delta_k + \omega_e)d/v_g} \right] \\ &= \frac{2g^2}{v_g} \int_0^\infty d\tau \left[\int_{-\infty}^{+\infty} d\delta_k e^{-i(\Delta_c + \delta_k)\tau} e^{\mp i(\delta_k + \omega_e)d/v_g} + \int_{-\infty}^{+\infty} d\delta_k e^{-i(\Delta_c + \delta_k)\tau} e^{\pm i(\delta_k + \omega_e)d/v_g} \right] \\ &= \frac{2g^2}{v_g} \left[e^{i(\omega_e d/v_g - \Delta_c \tau)} \int_0^\infty d\tau 2\pi \delta(\tau - d/v_g) + e^{-i(\omega_e d/v_g + \Delta_c \tau)} \int_0^\infty d\tau 2\pi \delta(\tau + d/v_g) \right] \\ &= \frac{4\pi g^2}{v_g} e^{i(\omega_e - \Delta_c)d/v_g} \simeq \frac{4\pi g^2}{v_g} e^{i\omega_e d/v_g} = \Gamma e^{i\phi}, \end{aligned} \quad (\text{B4})$$

as well as $\Gamma_{\text{ex}} = \text{Re}\{\tilde{\Gamma}\} = \Gamma \cos\phi$ and $J_{\text{ex}} = \text{Im}\{\tilde{\Gamma}\} = \Gamma \sin\phi$. In the above derivation, we have also considered the δ function definition $\int_{-\infty}^{+\infty} dke^{\pm ikx} = 2\pi \delta(x)$ and the waveguide mode density $D(k) = \partial k / \partial \omega_k$ [2,3,57].

Note that Eq. (B3) just describes the interactions between a continuum of waveguide modes and two lower atomic transitions $|g_1 g_2\rangle \leftrightarrow |g_1 r_2\rangle$ and $|g_1 g_2\rangle \leftrightarrow |r_1 g_2\rangle$. Further taking into account the intrinsic atomic decay toward nonguided modes in the free space as well as the neglected interactions between a coherent field and two upper atomic transitions $|g_1 r_2\rangle \leftrightarrow |r_1 r_2\rangle$ and $|r_1 g_2\rangle \leftrightarrow |r_1 r_2\rangle$ in H , one can easily obtain the master equation (2) in the main text. This equation, if expanded in the two-atom four-level configuration, will turn out to be

$$\begin{aligned} \partial_t \rho_{g_1 g_1, g_2 g_2} &= (\gamma + \Gamma) \rho_{r_1 r_1, g_2 g_2} + (\gamma + \Gamma) \rho_{g_1 g_1, r_2 r_2} + \Gamma_{\text{ex}} \rho_{r_1 g_1, g_2 r_2} + \Gamma_{\text{ex}} \rho_{g_1 r_1, r_2 g_2}, \\ \partial_t \rho_{r_1 r_1, g_2 g_2} &= -(\gamma + \Gamma) \rho_{r_1 r_1, g_2 g_2} + \gamma \rho_{r_1 r_1, r_2 r_2} - \tilde{\Gamma}/2 \rho_{g_1 r_1, r_2 g_2} - \tilde{\Gamma}^*/2 \rho_{r_1 g_1, g_2 r_2} - i(\Omega_c \rho_{r_1 r_1, g_2 r_2} - \Omega_c^* \rho_{r_1 r_1, r_2 g_2}), \\ \partial_t \rho_{g_1 g_1, r_2 r_2} &= -(\gamma + \Gamma) \rho_{g_1 g_1, r_2 r_2} + \gamma \rho_{r_1 r_1, r_2 r_2} - \tilde{\Gamma}/2 \rho_{r_1 g_1, g_2 r_2} - \tilde{\Gamma}^*/2 \rho_{g_1 r_1, r_2 g_2} - i(\Omega_c \rho_{g_1 r_1, r_2 g_2} - \Omega_c^* \rho_{r_1 g_1, r_2 r_2}), \\ \partial_t \rho_{g_1 r_1, g_2 g_2} &= (i\Delta_c - \gamma/2 - \Gamma/2) \rho_{g_1 r_1, g_2 g_2} + \gamma \rho_{g_1 r_1, r_2 r_2} - \tilde{\Gamma}^*/2 \rho_{g_1 g_1, g_2 r_2} - i\Omega_c \rho_{g_1 r_1, g_2 r_2}, \\ \partial_t \rho_{r_1 g_1, g_2 g_2} &= -(i\Delta_c + \gamma/2 + \Gamma/2) \rho_{r_1 g_1, g_2 g_2} + \gamma \rho_{r_1 g_1, r_2 r_2} - \tilde{\Gamma}/2 \rho_{g_1 g_1, r_2 g_2} + i\Omega_c^* \rho_{r_1 g_1, r_2 g_2}, \\ \partial_t \rho_{g_1 g_1, g_2 r_2} &= (i\Delta_c - \gamma/2 - \Gamma/2) \rho_{g_1 g_1, g_2 r_2} + \gamma \rho_{r_1 r_1, g_2 r_2} - \tilde{\Gamma}^*/2 \rho_{g_1 r_1, r_2 g_2} - i\Omega_c \rho_{g_1 r_1, g_2 r_2}, \\ \partial_t \rho_{r_1 g_1, r_2 g_2} &= -(i\Delta_c + \gamma/2 + \Gamma/2) \rho_{r_1 g_1, r_2 g_2} + \gamma \rho_{r_1 r_1, r_2 g_2} - \tilde{\Gamma}/2 \rho_{r_1 g_1, g_2 r_2} + i\Omega_c^* \rho_{r_1 g_1, r_2 g_2}, \\ \partial_t \rho_{g_1 r_1, g_2 r_2} &= -\gamma \rho_{g_1 r_1, g_2 r_2} - i\Omega_c^* (\rho_{g_1 r_1, g_2 g_2} + \rho_{g_1 g_1, g_2 r_2}), \\ \partial_t \rho_{r_1 g_1, r_2 g_2} &= -\gamma \rho_{r_1 g_1, r_2 g_2} + i\Omega_c (\rho_{r_1 g_1, g_2 g_2} + \rho_{g_1 g_1, r_2 g_2}), \end{aligned}$$

$$\begin{aligned}
\partial_t \rho_{r_1 g_1, g_2 r_2} &= -(\gamma + \Gamma) \rho_{r_1 g_1, g_2 r_2} - \tilde{\Gamma}/2 \rho_{g_1 g_1, r_2 r_2} - \tilde{\Gamma}^*/2 \rho_{r_1 r_1, g_2 g_2} - i(\Omega_c \rho_{r_1 r_1, g_2 r_2} - \Omega_c^* \rho_{r_1 g_1, r_2 r_2}), \\
\partial_t \rho_{g_1 r_1, r_2 g_2} &= -(\gamma + \Gamma) \rho_{g_1 r_1, r_2 g_2} - \tilde{\Gamma}^*/2 \rho_{g_1 g_1, r_2 r_2} - \tilde{\Gamma}/2 \rho_{r_1 r_1, g_2 g_2} + i(\Omega_c^* \rho_{r_1 r_1, r_2 g_2} - \Omega_c \rho_{g_1 r_1, r_2 r_2}), \\
\partial_t \rho_{r_1 r_1, g_2 r_2} &= -(i\Delta_c + 3\gamma/2 + \Gamma/2) \rho_{r_1 r_1, g_2 r_2} - \tilde{\Gamma}/2 \rho_{g_1 g_1, r_2 r_2} - i\Omega_c^* (\rho_{r_1 r_1, g_2 g_2} + \rho_{r_1 g_1, r_2 r_2} - \rho_{r_1 r_1, r_2 r_2}), \\
\partial_t \rho_{r_1 r_1, r_2 g_2} &= (i\Delta_c - 3\gamma/2 - \Gamma/2) \rho_{r_1 r_1, r_2 g_2} - \tilde{\Gamma}^*/2 \rho_{r_1 g_1, r_2 r_2} + i\Omega_c (\rho_{r_1 r_1, g_2 g_2} + \rho_{g_1 r_1, r_2 g_2} - \rho_{r_1 r_1, r_2 r_2}), \\
\partial_t \rho_{g_1 r_1, r_2 r_2} &= -(i\Delta_c + 3\gamma/2 + \Gamma/2) \rho_{g_1 r_1, r_2 r_2} - \tilde{\Gamma}/2 \rho_{r_1 r_1, g_2 r_2} - i\Omega_c^* (\rho_{g_1 r_1, r_2 g_2} + \rho_{g_1 g_1, r_2 r_2} - \rho_{r_1 r_1, r_2 r_2}), \\
\partial_t \rho_{r_1 g_1, r_2 r_2} &= (i\Delta_c - 3\gamma/2 - \Gamma/2) \rho_{r_1 g_1, r_2 r_2} - \tilde{\Gamma}^*/2 \rho_{r_1 r_1, r_2 g_2} + i\Omega_c (\rho_{r_1 g_1, g_2 r_2} + \rho_{g_1 g_1, r_2 r_2} - \rho_{r_1 r_1, r_2 r_2}),
\end{aligned} \tag{B5}$$

constrained by $\rho_{g_1 g_1, g_2 g_2} + \rho_{r_1 r_1, g_2 g_2} + \rho_{g_1 g_1, r_2 r_2} + \rho_{r_1 r_1, r_2 r_2} = 1$.

As mentioned in the main text, it is helpful to understand the long-time entanglement onset dynamics by replacing single-excitation states $|g_1 r_2\rangle$ and $|r_1 g_2\rangle$ with their superpositions $|\pm\rangle = 1/\sqrt{2}(|r_1 g_2\rangle \pm |g_1 r_2\rangle)$. Population evolutions in the two symmetric and antisymmetric states can be calculated from the above equations as

$$\begin{aligned}
\partial_t \rho_{++} &= \frac{1}{2} (\partial_t \rho_{g_1 g_1, r_2 r_2} + \partial_t \rho_{r_1 r_1, g_2 g_2} + \partial_t \rho_{r_1 g_1, g_2 r_2} + \partial_t \rho_{g_1 r_1, r_2 g_2}) \\
&= \frac{1}{2} [(-\gamma - \Gamma - \tilde{\Gamma}^*/2 - \tilde{\Gamma}/2) (\rho_{g_1 g_1, r_2 r_2} + \rho_{r_1 r_1, g_2 g_2} + \rho_{r_1 g_1, g_2 r_2} + \rho_{g_1 r_1, r_2 g_2}) + \gamma \rho_{r_1 r_1, r_2 r_2}] \\
&\quad + i(\Omega_c^* \rho_{r_1 r_1, r_2 g_2} + \Omega_c^* \rho_{r_1 g_1, r_2 r_2} - \Omega_c \rho_{r_1 r_1, g_2 r_2} - \Omega_c \rho_{g_1 r_1, r_2 r_2}) \\
&= -(\gamma + \Gamma + \Gamma_{ex}) \rho_{++} + \gamma \rho_{rr} + i\Omega_c^* \rho_{r+} - i\Omega_c \rho_{+r}, \\
\partial_t \rho_{--} &= \frac{1}{2} (\partial_t \rho_{g_1 g_1, r_2 r_2} + \partial_t \rho_{r_1 r_1, g_2 g_2} - \partial_t \rho_{r_1 g_1, g_2 r_2} - \partial_t \rho_{g_1 r_1, r_2 g_2}) \\
&= \frac{1}{2} [(-\gamma - \Gamma + \tilde{\Gamma}^*/2 + \tilde{\Gamma}/2) (\rho_{g_1 g_1, r_2 r_2} + \rho_{r_1 r_1, g_2 g_2} - \rho_{r_1 g_1, g_2 r_2} - \rho_{g_1 r_1, r_2 g_2}) + \gamma \rho_{r_1 r_1, r_2 r_2}] \\
&= -(\gamma + \Gamma - \Gamma_{ex}) \rho_{--} + \gamma \rho_{rr},
\end{aligned} \tag{B6}$$

which are exactly Eq. (8) in the main text if we further introduce $\gamma_{\pm} = \gamma + \Gamma \pm \Gamma_{ex}$.

APPENDIX C: MASTER EQUATION OF A GIANT-ATOM TWO-LEVEL CONFIGURATION

In the case that the single-excitation states $|r_1 g_2\rangle$ and $|g_1 r_2\rangle$ are not populated initially, if we have $|\Delta_c| \gg \Omega_c, g$ and $\Delta_c + \delta_k \simeq 0$, our two-atom four-level configuration can be reduced to a (synthetic) giant-atom two-level configuration by eliminating $|r_1 g_2\rangle$ and $|g_1 r_2\rangle$ in the *short-time* regime. In view of this, a pair of Rydberg atoms will decay from the double-excitation state $|r_1 r_2\rangle$ directly to the ground state $|g_1 g_2\rangle$ by simultaneously emitting a coherent-field photon of frequency ω_c and a waveguide-mode photon of frequency ω_k , through two competing two-photon resonant transitions exhibiting effective coupling strengths $\xi_1 = -g\Omega_c/\Delta_c \equiv \xi$ and $\xi_2 = \xi e^{i\phi}$, respectively. This can be substantiated by the following discussions starting from an *effective* Hamiltonian defined as [46,58]

$$H_e(t) = -iH_I(t) \int_0^t H_I(t') dt', \tag{C1}$$

with

$$H_I(t) = \int dk g a_k e^{-i\delta_k t} (\sigma_+^1 + e^{ikd} \sigma_+^2) + \Omega_c e^{-i\Delta_c t} (\sigma_+^3 + \sigma_+^4) + \text{H.c.} \tag{C2}$$

being the total interaction Hamiltonian involving both waveguide modes and coherent field of our two-atom four-level configuration. Substituting Eq. (C2) into Eq. (C1), one has

$$\begin{aligned}
H_e(t) &\simeq \frac{g^2}{\delta_k} \int dka_k a_k^\dagger (\sigma_-^1 \sigma_+^1 + \sigma_-^2 \sigma_+^2) - \frac{\Omega_c^2}{\Delta_c} (\sigma_+^3 \sigma_-^3 + \sigma_+^4 \sigma_-^4) \\
&\quad + \frac{g\Omega_c}{\delta_k} \int dka_k e^{-i(\delta_k + \Delta_c)t} (\sigma_+^3 \sigma_+^1 + e^{ikd} \sigma_+^4 \sigma_+^2) - \frac{g\Omega_c}{\Delta_c} \int dka_k^\dagger e^{i(\delta_k + \Delta_c)t} (\sigma_-^1 \sigma_-^3 + e^{-ikd} \sigma_-^2 \sigma_-^4) + \dots \\
&= \frac{2g^2}{\delta_k} \int dka_k a_k^\dagger |g_1 g_2\rangle \langle g_1 g_2| - \frac{2\Omega_c^2}{\Delta_c} |r_1 r_2\rangle \langle r_1 r_2| \\
&\quad + \frac{g\Omega_c}{\delta_k} \int dka_k e^{-i(\delta_k + \Delta_c)t} (1 + e^{ikd}) |r_1 r_2\rangle \langle g_1 g_2| - \frac{g\Omega_c}{\Delta_c} \int dka_k^\dagger e^{i(\delta_k + \Delta_c)t} (1 + e^{-ikd}) |g_1 g_2\rangle \langle r_1 r_2| + \dots,
\end{aligned} \tag{C3}$$

where we have omitted a few terms related to the single-excited states $|r_1 g_2\rangle$ and $|g_1 r_2\rangle$ since they are decoupled from other states and only interact with each other.

Considering again $\Delta_c + \delta_k \simeq 0$ and $|\Delta_c| \gg \Omega_c$, g as mentioned above, we have $|g^2/\delta_k| \rightarrow 0$ and $|\Omega_c^2/\Delta_c| \rightarrow 0$, which then result in a reduction of H_e into the interaction Hamiltonian

$$\mathcal{H}_{\text{int}}(t) = \int_{-\infty}^{+\infty} dk [\xi(1 + e^{ikd})e^{-i(\delta_k + \Delta_c)t} a_k \sigma_+ + \text{H.c.}], \quad (\text{C4})$$

for a synthetic giant atom with two levels $|g\rangle = |g_1 g_2\rangle$ and $|r\rangle = |r_1 r_2\rangle$ by taking $\xi = g\Omega_c/\delta_k = -g\Omega_c/\Delta_c$. We can attain \mathcal{H} in Eq. (4) of the main text by rotating this interaction Hamiltonian with respect to frequency $2\omega_e + V_6$ of the giant-atom transition $|g\rangle \leftrightarrow |r\rangle$, which is coupled to a continuum of waveguide modes of frequency ω_k accompanied by a coherent field of frequency ω_c . Substituting Eq. (C4) into an equation similar to Eq. (B2) for the giant-atom density operator ρ , we can further attain the master equation (5) in the main text by including also the intrinsic atomic decay toward nonguided modes in the free space. This master equation turns out to be

$$\begin{aligned} \partial_t \rho_{gg} &= (\Upsilon + \Upsilon^* + 2\gamma)\rho_{rr}, \\ \partial_t \rho_{gr} &= -(\Upsilon^* + \gamma)\rho_{gr}, \\ \partial_t \rho_{rg} &= -(\Upsilon + \gamma)\rho_{rg}, \end{aligned} \quad (\text{C5})$$

after an expansion in the giant-atom two-level configuration and are constrained by $\rho_{gg} + \rho_{rr} = 1$ with

$$\Upsilon = 2\xi^2 \int_0^\infty d\tau \int_{-\infty}^{+\infty} dk [e^{\pm i(\delta_k + \Delta_c)\tau} + e^{-i(\delta_k + \Delta_c)\tau} e^{\pm ikd}] = 4\pi\xi^2 D(k)[1 + e^{i\phi}] = (\Gamma + \Gamma_{ex} + iJ_{ex})\Omega_c^2/\Delta_c^2. \quad (\text{C6})$$

APPENDIX D: CONTINUOUS COUPLINGS OF RYDBERG ATOMS AND WAVEGUIDE MODES

In this section, we try to derive the explicit expressions of relevant constants describing various interactions between two Rydberg atoms and a continuum of waveguide modes modified in the case of continuous couplings. As shown in Fig. 4(a) in the main text, the two continuous couplings around $x_1 = 0$ and $x_2 = d$ exhibit a common characteristic width Θ , with which relevant exponential distribution functions can be expressed as $v_1(\varphi) = \frac{\sqrt{\Gamma}}{\Theta} e^{-\frac{2}{\Theta}|\varphi|}$ and $v_2(\varphi) = \frac{\sqrt{\Gamma}}{\Theta} e^{-\frac{2}{\Theta}|\varphi - \phi|}$ that satisfy $\int d\varphi v_{1,2}(\varphi) = \sqrt{\Gamma}$ [4]. Here $\varphi = \phi x/d \simeq \omega_e x/v_g$ describes the phase accumulated from x_1 to x by a propagating photon along the waveguide and will become ϕ in the case of $x = x_2$, which has been considered above for two discrete couplings. In this way, one can immediately generalize the master equation (2) in the main text to the continuous-coupling case, where the modified constants are given by

$$\begin{aligned} \Gamma' &= \int_{-\infty}^{\infty} d\varphi \int_{-\infty}^{\infty} d\varphi' v_1(\varphi) v_1(\varphi') \cos(\varphi - \varphi') \\ &= \frac{\Gamma}{\Theta^2} \int_{-\infty}^{\infty} d\varphi \int_{-\infty}^{\infty} d\varphi' e^{-\frac{2}{\Theta}|\varphi|} e^{-\frac{2}{\Theta}|\varphi'|} \cos(\varphi - \varphi') \\ &= \frac{\Gamma}{\Theta^2} \left[\int_0^\infty d\varphi \int_0^\infty d\varphi' e^{-\frac{2}{\Theta}\varphi} e^{-\frac{2}{\Theta}\varphi'} \cos(\varphi - \varphi') + \int_0^\infty d\varphi \int_{-\infty}^0 d\varphi' e^{-\frac{2}{\Theta}\varphi} e^{\frac{2}{\Theta}\varphi'} \cos(\varphi - \varphi') \right. \\ &\quad \left. + \int_{-\infty}^0 d\varphi \int_0^\infty d\varphi' e^{\frac{2}{\Theta}\varphi} e^{-\frac{2}{\Theta}\varphi'} \cos(\varphi - \varphi') + \int_{-\infty}^0 d\varphi \int_{-\infty}^0 d\varphi' e^{\frac{2}{\Theta}\varphi} e^{\frac{2}{\Theta}\varphi'} \cos(\varphi - \varphi') \right] \\ &= \frac{16\Gamma}{(\Theta^2 + 4)^2}, \end{aligned} \quad (\text{D1})$$

$$\begin{aligned} J'_{ex} &= \int_{-\infty}^{\infty} d\varphi \int_{-\infty}^{\infty} d\varphi' v_1(\varphi) v_2(\varphi') \sin|\varphi - \varphi'| \\ &= \frac{\Gamma}{\Theta^2} \int_{-\infty}^{\infty} d\varphi \int_{-\infty}^{\infty} d\varphi' e^{-\frac{2}{\Theta}|\varphi|} e^{-\frac{2}{\Theta}|\varphi' - \phi|} \sin|\varphi - \varphi'| \\ &= \frac{\Gamma}{\Theta^2} \left[2 \int_\phi^\infty d\varphi \int_\phi^\varphi d\varphi' e^{-\frac{2}{\Theta}\varphi} e^{-\frac{2}{\Theta}(\varphi' - \phi)} \sin(\varphi - \varphi') + \int_\phi^\infty d\varphi \int_0^\phi d\varphi' e^{-\frac{2}{\Theta}\varphi} e^{\frac{2}{\Theta}(\varphi' - \phi)} \sin(\varphi - \varphi') \right. \\ &\quad \left. + \int_\phi^\infty d\varphi \int_{-\infty}^0 d\varphi' e^{-\frac{2}{\Theta}\varphi} e^{\frac{2}{\Theta}(\varphi' - \phi)} \sin(\varphi - \varphi') + \int_0^\phi d\varphi \int_\phi^\infty d\varphi' e^{-\frac{2}{\Theta}\varphi} e^{-\frac{2}{\Theta}(\varphi' - \phi)} \sin(\varphi - \varphi') \right. \\ &\quad \left. + \int_0^\phi d\varphi \int_0^\varphi d\varphi' e^{-\frac{2}{\Theta}\varphi} e^{\frac{2}{\Theta}(\varphi' - \phi)} \sin(\varphi - \varphi') + \int_0^\phi d\varphi' \int_0^{\varphi'} d\varphi e^{-\frac{2}{\Theta}\varphi} e^{\frac{2}{\Theta}(\varphi' - \phi)} \sin(\varphi' - \varphi) \right] \end{aligned}$$

$$\begin{aligned}
& + \int_0^\phi d\varphi \int_{-\infty}^0 d\varphi' e^{-\frac{2}{\Theta}\varphi} e^{\frac{2}{\Theta}(\varphi'-\phi)} \sin(\varphi - \varphi') + \int_{-\infty}^0 d\varphi \int_\phi^\infty d\varphi' e^{\frac{2}{\Theta}\varphi} e^{-\frac{2}{\Theta}(\varphi'-\phi)} \sin(\varphi' - \varphi) \\
& + \int_{-\infty}^0 d\varphi \int_0^\phi d\varphi' e^{\frac{2}{\Theta}\varphi} e^{\frac{2}{\Theta}(\varphi'-\phi)} \sin(\varphi' - \varphi) + 2 \int_{-\infty}^0 d\varphi \int_{-\infty}^\phi d\varphi' e^{\frac{2}{\Theta}\varphi} e^{\frac{2}{\Theta}(\varphi'-\phi)} \sin(\varphi - \varphi') \Big] \\
& = \frac{\Gamma}{(\Theta^2 + 4)^2} [(8\phi + 2\Theta^2\phi + 12\Theta + \Theta^3)e^{-\frac{2\phi}{\Theta}} + 16\sin\phi], \tag{D2} \\
\Gamma'_{ex} & = \int_{-\infty}^\infty d\varphi \int_{-\infty}^\infty d\varphi' v_1(\varphi)v_2(\varphi')\cos(\varphi - \varphi') \\
& = \frac{\Gamma}{\Theta^2} \left[\int_0^\infty d\varphi \int_\phi^\infty d\varphi' e^{-\frac{2}{\Theta}\varphi} e^{-\frac{2}{\Theta}(\varphi'-\phi)} \cos(\varphi - \varphi') + \int_0^\infty d\varphi \int_{-\infty}^\phi d\varphi' e^{-\frac{2}{\Theta}\varphi} e^{\frac{2}{\Theta}(\varphi'-\phi)} \cos(\varphi - \varphi') \right. \\
& \quad \left. + \int_{-\infty}^0 d\varphi \int_\phi^\infty d\varphi' e^{\frac{2}{\Theta}\varphi} e^{-\frac{2}{\Theta}(\varphi'-\phi)} \cos(\varphi - \varphi') + \int_{-\infty}^0 d\varphi \int_{-\infty}^\phi d\varphi' e^{\frac{2}{\Theta}\varphi} e^{\frac{2}{\Theta}(\varphi'-\phi)} \cos(\varphi - \varphi') \right] \\
& = \frac{16\Gamma\cos\phi}{(\Theta^2 + 4)^2}, \tag{D3}
\end{aligned}$$

with $\varphi' = \phi x'/v_g$ for a position x' different from x . Moreover, an extra coherent interaction term $\sum_{j=1,2} J' \sigma_+^j \sigma_-^j$ has to be introduced in H_{at} with the effective interaction strength obtained as

$$\begin{aligned}
J' & = \int_{-\infty}^\infty d\varphi \int_{-\infty}^\infty d\varphi' v_1(\varphi)v_1(\varphi')\sin|\varphi - \varphi'| \\
& = \frac{\Gamma}{\Theta^2} \int_{-\infty}^\infty d\varphi \int_{-\infty}^\infty d\varphi' e^{-\frac{2}{\Theta}|\varphi|} e^{-\frac{2}{\Theta}|\varphi'|} \sin|\varphi - \varphi'| \\
& = \frac{\Gamma}{\Theta^2} \left[2 \int_0^\infty d\varphi \int_0^\varphi d\varphi' e^{-\frac{2}{\Theta}\varphi} e^{-\frac{2}{\Theta}\varphi'} \sin(\varphi - \varphi') + \int_0^\infty d\varphi \int_{-\infty}^0 d\varphi' e^{-\frac{2}{\Theta}\varphi} e^{\frac{2}{\Theta}\varphi'} \sin(\varphi - \varphi') \right. \\
& \quad \left. + \int_{-\infty}^0 d\varphi \int_0^\infty d\varphi' e^{\frac{2}{\Theta}\varphi} e^{-\frac{2}{\Theta}\varphi'} \sin(\varphi' - \varphi) + 2 \int_{-\infty}^0 d\varphi \int_{-\infty}^\varphi d\varphi' e^{\frac{2}{\Theta}\varphi} e^{\frac{2}{\Theta}\varphi'} \sin(\varphi - \varphi') \right] \\
& = \frac{\Gamma\Theta(\Theta^2 + 12)}{(\Theta^2 + 4)^2}. \tag{D4}
\end{aligned}$$

Note also that the expressions of J' and Γ' will remain unchanged if we replace v_1 by v_2 , i.e.,

$$\int_{-\infty}^\infty d\varphi \int_{-\infty}^\infty d\varphi' v_1(\varphi)v_1(\varphi')e^{i|\varphi-\varphi'|} = \int_{-\infty}^\infty d\varphi \int_{-\infty}^\infty d\varphi' v_2(\varphi)v_2(\varphi')e^{i|\varphi-\varphi'|}, \tag{D5}$$

implying that the two constants are identical for both Rydberg atoms.

For the synthetic two-level giant atom, in a similar way, $\Upsilon = (\Gamma + \Gamma_{ex} + iJ_{ex})\Omega_c^2/\Delta_c^2$ in the case of discrete couplings should be replaced by $\Upsilon' = (\Gamma' + \Gamma'_{ex} + iJ' + iJ'_{ex})\Omega_c^2/\Delta_c^2$ in the case of continuous couplings.

Finally, we discuss how to control the coupling characteristic width Θ in experiment by considering the radial size \bar{r} of a Rydberg atom. To be more specific, this characteristic width can be estimated as $\Theta = w\omega_e/v_g = 2\sqrt{\bar{r}^2 - h^2}\omega_e/v_g$ with w being the overlap width between the electronic wavefunction of the Rydberg atom and the evanescent field of the waveguide while h the distance from the Rydberg-atom nucleus to the evanescent-field surface. Then it is viable to attain $\Theta = 5\pi/2$ with $h \simeq 449$ nm since we have $\bar{r} \simeq 583$ nm for $|r_{1,2}\rangle = |75P_{3/2}\rangle$ [48].

-
- [1] A. F. Kockum, Quantum optics with giant atoms—The first five years, in *Mathematics for Industry* (Springer, Singapore, 2021), pp. 125–146.
- [2] A. F. Kockum, P. Delsing, and G. Johansson, Designing frequency-dependent relaxation rates and Lamb shifts for a giant artificial atom, *Phys. Rev. A* **90**, 013837 (2014).
- [3] B. Kannan, M. Ruckriegel, D. Campbell, A. F. Kockum, J. Braumüller, D. Kim, M. Kjaergaard, P. Krantz, A. Melville, B. M. Niedzielski *et al.*, Waveguide quantum electrodynamics

with superconducting artificial giant atoms, *Nature (London)* **583**, 775 (2020).

- [4] Q. Y. Cai and W. Z. Jia, Coherent single-photon scattering spectra for a giant-atom waveguide-QED system beyond the dipole approximation, *Phys. Rev. A* **104**, 033710 (2021).
- [5] Y. T. Chen, L. Du, L. Guo, Z. Wang, Y. Zhang, Y. Li, and J. H. Wu, Nonreciprocal and chiral single-photon scattering for giant atoms, *Commun. Phys.* **5**, 215 (2022).

- [6] X.-L. Yin, Y.-H. Liu, J.-F. Huang, and J.-Q. Liao, Single-photon scattering in a giant-molecule waveguide-QED system, *Phys. Rev. A* **106**, 013715 (2022).
- [7] L. Guo, A. L. Grimsmo, A. F. Kockum, M. Pletyukhov, and G. Johansson, Giant acoustic atom: A single quantum system with a deterministic time delay, *Phys. Rev. A* **95**, 053821 (2017).
- [8] G. Andersson, B. Suri, L. Guo, T. Aref, and P. Delsing, Nonexponential decay of a giant artificial atom, *Nat. Phys.* **15**, 1123 (2019).
- [9] Q.-Y. Qiu, Y. Wu, and X.-Y. Lü, Collective radiance of giant atoms in non-Markovian regime, *Sci. China Phys. Mech. Astron.* **66**, 224212 (2023).
- [10] A. F. Kockum, G. Johansson, and F. Nori, Decoherence-free interaction between giant atoms in waveguide quantum electrodynamics, *Phys. Rev. Lett.* **120**, 140404 (2018).
- [11] A. Carollo, D. Cilluffo, and F. Ciccarello, Mechanism of decoherence-free coupling between giant atoms, *Phys. Rev. Res.* **2**, 043184 (2020).
- [12] A. Soro and A. F. Kockum, Chiral quantum optics with giant atoms, *Phys. Rev. A* **105**, 023712 (2022).
- [13] L. Guo, A. F. Kockum, F. Marquardt, and G. Johansson, Oscillating bound states for a giant atom, *Phys. Rev. Res.* **2**, 043014 (2020).
- [14] X. Wang, T. Liu, A. F. Kockum, H.-R. Li, and F. Nori, Tunable chiral bound states with giant atoms, *Phys. Rev. Lett.* **126**, 043602 (2021).
- [15] W. Zhao and Z. Wang, Single-photon scattering and bound states in an atom-waveguide system with two or multiple coupling points, *Phys. Rev. A* **101**, 053855 (2020).
- [16] H. Xiao, L. Wang, Z.-H. Li, X. Chen, and L. Yuan, Bound state in a giant atom-modulated resonators system, *npj Quantum Inf.* **8**, 80 (2022).
- [17] D. D. Noachtar, J. Knörzner, and R. H. Jonsson, Nonperturbative treatment of giant atoms using chain transformations, *Phys. Rev. A* **106**, 013702 (2022).
- [18] K. H. Lim, W.-K. Mok, and L.-C. Kwek, Oscillating bound states in non-Markovian photonic lattices, *Phys. Rev. A* **107**, 023716 (2023).
- [19] M. V. Gustafsson, T. Aref, A. F. Kockum, M. K. Ekström, G. Johansson, and P. Delsing, Propagating phonons coupled to an artificial atom, *Science* **346**, 207 (2014).
- [20] A. M. Vadiraj, A. Ask, T. G. McConkey, I. Nsanzeza, C. W. Sandbo Chang, A. F. Kockum, and C. M. Wilson, Engineering the level structure of a giant artificial atom in waveguide quantum electrodynamics, *Phys. Rev. A* **103**, 023710 (2021).
- [21] S. Longhi, Photonic simulation of giant atom decay, *Opt. Lett.* **45**, 3017 (2020).
- [22] A. González-Tudela, C. Sánchez Muñoz, and J. I. Cirac, Engineering and harnessing giant atoms in high-dimensional baths: A proposal for implementation with cold atoms, *Phys. Rev. Lett.* **122**, 203603 (2019).
- [23] L. Du, Y. Zhang, J.-H. Wu, A. F. Kockum, and Y. Li, Giant atoms in synthetic frequency dimensions, *Phys. Rev. Lett.* **128**, 223602 (2022).
- [24] Z. Q. Wang, Y. P. Wang, J. Yao, R. C. Shen, W. J. Wu, J. Qian, J. Li, S. Y. Zhu, and J. Q. You, Giant spin ensembles in waveguide magnonics, *Nat. Commun.* **13**, 7580 (2022).
- [25] M. Saffman, T. G. Walker, and K. Mølmer, Quantum information with Rydberg atoms, *Rev. Mod. Phys.* **82**, 2313 (2010).
- [26] D. Møller, L. B. Madsen, and K. Mølmer, Quantum gates and multiparticle entanglement by Rydberg excitation blockade and adiabatic passage, *Phys. Rev. Lett.* **100**, 170504 (2008).
- [27] D. Tiarks, S. Schmidt-Eberle, T. Stolz, G. Rempe, and S. Dürr, A photon-photon quantum gate based on Rydberg interactions, *Nat. Phys.* **15**, 124 (2019).
- [28] M. Khazali and K. Mølmer, Fast multiqubit gates by adiabatic evolution in interacting excited-state manifolds of Rydberg atoms and superconducting circuits, *Phys. Rev. X* **10**, 021054 (2020).
- [29] K. McDonnell, L. F. Keary, and J. D. Pritchard, Demonstration of a quantum gate using electromagnetically induced transparency, *Phys. Rev. Lett.* **129**, 200501 (2022).
- [30] D. Petrosyan and K. Mølmer, Deterministic free-space source of single photons using Rydberg atoms, *Phys. Rev. Lett.* **121**, 123605 (2018).
- [31] F. Ripka, H. Kübler, R. Löw, and T. Pfau, A room-temperature single-photon source based on strongly interacting Rydberg atoms, *Science* **362**, 446 (2018).
- [32] D. P. Ornelas-Huerta, A. N. Craddock, E. A. Goldschmidt, A. J. Hachtel, Y. Wang, P. Bienias, A. V. Gorshkov, S. L. Rolston, and J. V. Porto, On-demand indistinguishable single photons from an efficient and pure source based on a Rydberg ensemble, *Optica* **7**, 813 (2020).
- [33] S. Shi, B. Xu, K. Zhang, G.-S. Ye, D.-S. Xiang, Y. Liu, J. Wang, D. Su, and L. Li, High-fidelity photonic quantum logic gate based on near-optimal Rydberg single-photon source, *Nat. Commun.* **13**, 4454 (2022).
- [34] D. D. Bhaktavatsala Rao and K. Mølmer, Dark entangled steady states of interacting Rydberg atoms, *Phys. Rev. Lett.* **111**, 033606 (2013).
- [35] H. Levine, A. Keesling, A. Omran, H. Bernien, S. Schwartz, A. S. Zibrov, M. Endres, M. Greiner, V. Vuletić, and M. D. Lukin, High-fidelity control and entanglement of Rydberg-atom qubits, *Phys. Rev. Lett.* **121**, 123603 (2018).
- [36] I. S. Madjarov, J. P. Covey, A. L. Shaw, J. Choi, A. Kale, A. Cooper, H. Pichler, V. Schkolnik, J. R. Williams, and M. Endres, High-fidelity entanglement and detection of alkaline-earth Rydberg atoms, *Nat. Phys.* **16**, 857 (2020).
- [37] P.-F. Sun, Y. Yu, Z.-Y. An, J. Li, C.-W. Yang, X.-H. Bao, and J.-W. Pan, Deterministic time-bin entanglement between a single photon and an atomic ensemble, *Phys. Rev. Lett.* **128**, 060502 (2022).
- [38] K. S. Rajasree, T. Ray, K. Karlsson, J. L. Everett, and S. N. Chormaic, Generation of cold Rydberg atoms at submicron distances from an optical nanofiber, *Phys. Rev. Res.* **2**, 012038 (2020).
- [39] Y. Chougale, J. Talukdar, T. Ramos, and R. Nath, Dynamics of Rydberg excitations and quantum correlations in an atomic array coupled to a photonic crystal waveguide, *Phys. Rev. A* **102**, 022816(R) (2020).
- [40] S. D. Hogan, J. A. Agner, F. Merkt, T. Thiele, S. Philipp, and A. Wallraff, Driving Rydberg-Rydberg transitions from a coplanar microwave waveguide, *Phys. Rev. Lett.* **108**, 063004 (2012).
- [41] J. S. Douglas, H. H. Habibian, C.-L. Hung, A. V. Gorshkov, H. J. Kimble, and D. E. Chang, Quantum many-body models with cold atoms coupled to photonic crystals, *Nat. Photon.* **9**, 326 (2015).

- [42] J. D. Hood, A. Goban, A. Asenjo-Garcia, M. Lu, S.-P. Yu, D. E. Chang, and H. J. Kimble, Atom-atom interactions around the band edge of a photonic crystal waveguide, *Proc. Natl. Acad. Sci. USA* **113**, 10507 (2016).
- [43] H. Breuer and F. Petruccione, *The Theory of Open Quantum Systems* (Oxford University Press, Oxford, 2002).
- [44] G. Calajó, F. Ciccarello, D. Chang, and P. Rabl, Atom-field dressed states in slow-light waveguide QED, *Phys. Rev. A* **93**, 033833 (2016).
- [45] E. Brion, L. H. Pedersen, and K. Mølmer, Adiabatic elimination in a lambda system, *J. Phys. A: Math. Theor.* **40**, 1033 (2007).
- [46] D. Yan, J.-W. Gao, Q.-Q. Bao, H. Yang, H. Wang, and J.-H. Wu, Electromagnetically induced transparency in a five-level Λ system dominated by two-photon resonant transitions, *Phys. Rev. A* **83**, 033830 (2011).
- [47] I. I. Beterov, I. I. Ryabtsev, D. B. Tretyakov, and V. M. Entin, Quasiclassical calculations of blackbody-radiation-induced depopulation rates and effective lifetimes of Rydberg nS, nP, and nD alkali-metal atoms with $n \leq 80$, *Phys. Rev. A* **79**, 052504 (2009).
- [48] N. Šibalić, J. D. Pritchard, C. S. Adams, and K. J. Weatherill, An introduction to Rydberg atoms with ARC, available online at <https://arc-alkali-rydberg-calculator.readthedocs.io/en/latest/Rydberg-atoms-a-primer-notebook.html>.
- [49] W. K. Wootters, Entanglement of formation of an arbitrary state of two qubits, *Phys. Rev. Lett.* **80**, 2245 (1998).
- [50] K. M. O'connor and W. K. Wootters, Entangled rings, *Phys. Rev. A* **63**, 052302 (2001).
- [51] A. C. Santos and R. Bachelard, Generation of maximally entangled long-lived states with giant atoms in a waveguide, *Phys. Rev. Lett.* **130**, 053601 (2023).
- [52] J. von Zanthier, T. Bastin, and G. S. Agarwal, Measurement-induced spatial modulation of spontaneous decay and photon arrival times, *Phys. Rev. A* **74**, 061802(R) (2006).
- [53] J. Gillet, G. S. Agarwal, and T. Bastin, Tunable entanglement, antibunching, and saturation effects in dipole blockade, *Phys. Rev. A* **81**, 013837 (2010).
- [54] T. E. Lee, H. Häffner, and M. C. Cross, Collective quantum jumps of Rydberg atoms, *Phys. Rev. Lett.* **108**, 023602 (2012).
- [55] F. de Fornel, *Evanescent Waves from Newtonian Optics to Atomic Optics* (Springer-Verlag, Berlin, 2001).
- [56] Provided a crosstalk is avoided by keeping inter-pair distances sufficiently larger than intrapair distances.
- [57] S. Longhi, Quantum decay and amplification in a non-Hermitian unstable continuum, *Phys. Rev. A* **93**, 062129 (2016).
- [58] D. F. James and J. Jerke, Effective Hamiltonian theory and its applications in quantum information, *Can. J. Phys.* **85**, 625 (2007).